euspen's 21st International Conference & Exhibition, Copenhagen, DK, June 2021
www.euspen.eu

# Influence of ignition and polishing phase on jet shape and electric current in Jet-Plasma electrolytic Polishing

Susanne Quitzke[1], André Martin[1], Andreas Schubert[1]

[1]*Chemnitz University of Technology, Institute for Machine Tools and Production Processes, Professorship Micromanufacturing Technology, 09107 Chemnitz, Germany*

*email address: susanne.quitzke@mb.tu-chemnitz.de*

**Abstract**

Stainless steel AISI 316 L is frequently used as a material for medical applications such as surgery instruments, where polished surfaces are often required to achieve sufficient cleaning effects. In addition, polished surfaces are known to increase resistance against corrosion. Electrochemical polishing allows for surface treatment without mechanical nor thermal influences on the workpiece material, which is advantageous when handling filigree features on microsurgery instruments. Particularly, Plasma electrolytic Polishing (PeP) combines these advantages with a low material removal rate and is therefore applicable for precise post-processing of surfaces by immersing the workpieces into an electrolyte bath. Jet - Plasma electrolytic Polishing (Jet-PeP) offers the possibility for localized machining and leads to a reduced energy consumption compared to the immersion-based process, since only required surface areas are addressed. However, the physical-chemical process is not completely understood, yet.

Thus, the present investigation is focused on the analysis of the geometry of the electrolyte jet in Jet-PeP by optical detections with a high-speed camera and its influence on the resulting removal area. The captured images were synchronized with the electrical current measured during Jet-PeP of stainless steel AISI 316 L. The diameter and shape of the electrolyte jet formed on a planar workpiece surface was analysed before and during the process. The process itself was classified into two phases. The first phase was characterised by a current peak up to 22 A leading to a widening followed by an interruption of the electrolyte jet due to the formation of gas bubbles. The subsequent second phase was characterized by stochastic current peaks up to 5 A in a time duration between 0.03 s to 0.06 s caused by electrical discharges and interruptions of the contact between electrolyte jet and metal surface.

keywords: Jet-PeP, localized plasma electrolytic polishing, highspeed imaging, current peaks

## 1. Introduction

Stainless steels are used for several applications, in which high corrosion resistance and high stiffness are required. A typical stainless steel for medical applications is AISI 316 L (1.4404), which offers sufficiently high creep strain, high failure stress and high tensile strength. Moreover, AISI 316 L provides an excellent machineability and formability [1].

One exemplary application of AISI 316 L are tube coronary stents, which can be smoothened by electrochemical polishing without mechanical nor thermal influences. [2]. Loaldi et al. [3] compared different post-processing methods for the additive manufactured metal AISI 316 L and determined that with Plasma electrolytic Polishing (PeP) the average roughness can be reduced to values below 1 µm. Additionally, the plaque concentration was lower and the cell mortality was not significantly increased after polishing the surface [4].

This indicates the high relevance of PeP for post-processing of stainless-steel parts for medical applications.

## 2. State of the art of Plasma electrolytic Polishing

PeP is based on the immersion of the workpiece (anode) into an electrolyte bath (cathode), which is composed of an aqueous, environmentally friendly electrolyte, at voltages in the range from 180 V to 300 V when polishing stainless steel. A gaseous layer is formed on the surrounding workpiece surface and the material is removed by a chemical-physical process [5]. At the beginning of the PeP process, the electrical current raises up to a maximum and decreases exponentially during the processing time. The values depend on the processing parameters and the initial workpiece surface [6].

Jet-based Plasma electrolytic Polishing (Jet-PeP) is a specific further development of PeP, where a cathodically polarized nozzle is used to apply a closed electrolytic free jet towards the anodically polarized workpiece. The electrolyte jet hits the workpiece surface orthogonally. A kinematic system is used for the positioning of the nozzle and adjustment of the distance between nozzle and workpiece. Hence, Jet-PeP allows for local polishing of selective areas and properties of the surrounding metal surface are not changed [7].

Akhatov et al. [8] determined an electric current in the range from 0.1 A to 1.5 A for a diameter of the jet in the range from 1 mm to 10 mm. According to Popov et al. [9] the electric current increased until a voltage of 300 V and was defined as electrolysis mode. With further increase of the voltage at 400 V and 500 V the electric current was nearly constant and marks the electrolyte-plasma discharge mode.

The shape of the electrolyte jet during the process depends on the applied voltage and the distribution of electric field. Following shapes are classified: hemisphere, cylinder, hyperboloid and truncated ellipsoid [9].

Due to the electric discharges in the electrolyte jet, current peaks were detected during the process [10]. The current peaks were characterized by amplitudes of 2.4 A and pulse times between 3 ms and 9 ms [11]. The discharges lead to local temperature increase in the electrolyte jet up to 100 °C. Nevertheless, the temperature of the workpiece remains in the range of 45 °C to 95 °C [11]. Additionally, the electric discharges lead to shock waves in the electrolyte jet [12]. These lead to

intensive evaporation of the electrolyte and the electrolyte gets a deformed surface [13].

Probably, the luminescence of the electrolyte jet during the process is caused by ion recombination [9] that arises by the high polarization and collision of ions in the gaseous layer [14].

According to the current state-of-the-art, the Jet-PeP process is characterized by electric current peaks, various shapes of the electrolyte jet and luminescence. By using a high-speed camera and measuring electric current characteristics along with the comparison to theoretical calculations, the process is described more in detail in this study to allow for a deeper understanding of the Jet-PeP process.

## 3. Experimental setup and parameters

The experiments were carried out on the Jet-PeP setup shown in the schematic of Figure 1.

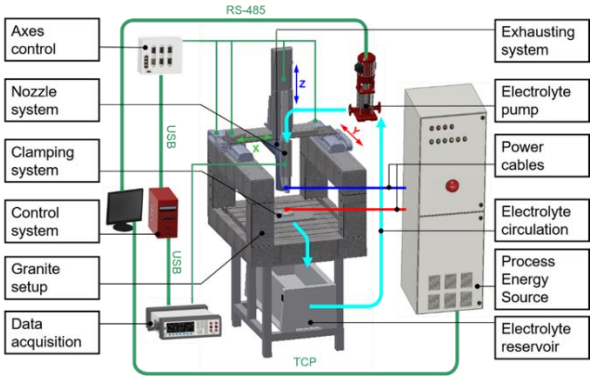


**Figure 1.** Schematic of the Jet-PeP setup [15].

The setup consists of a control system, data acquisition, kinematic system, electrical system, process chamber and electrolyte system [15]. The electric current between the cathodically polarized nozzle and the anodically polarized workpiece is measured over a shunt resistor with digital multimeters (Keysight 34465 A) and recorded into protocol files with a custom control software based on LabVIEW from National Instruments. A specific process energy source for Jet-PeP developed by Leukhardt Schaltanlagen Systemtechnik GmbH, Magdeburg, Germany, was used.

AISI 316 L was used as sample material. Jet-PeP experiments were carried out on a planar surface that was cleaned up with acetone and deionized water before the experiments. Table 1 presents the process parameters.

**Table 1** Jet-PeP processing parameters.

| Parameter | Value |
|---|---|
| Voltage | 300 V, 400 V, 500 V, 600 V |
| Nozzle diameter | 5 mm |
| Working gap | 6 mm, 10 mm |
| Electrolyte flow rate | 200 ml/min, 250 ml/min |
| Electrolyte type and concentration | ammonium sulfate, 5 wt.-% |
| Electrolyte temperature | 80 °C |
| Electrolyte conductivity | 108 mS/cm |

A compressed air support with 0.2 bar was used to push away accumulations of electrolyte on the workpiece surface and to realize the formation of an electrolytic free jet.

For the optical investigations of the process, a high-speed camera FASTCAM AX200 model 900K-M-32 GB of the company Photron with 2,000 fps was used. Integrated LED lamps were used for the illumination of the processing zone. A white plastic plate was placed in the background to provide enough light for the optical investigations. The distance between the process zone and the objective of the high-speed camera was set to 350 mm.

For the determination of the required electric current at the beginning of the process, the resistance of the electrolyte jet $R_{\mathrm{Jet}}$ was calculated according to equation (1)

$$R_{\mathrm{Jet}} = \frac{1}{\kappa} \cdot \frac{s}{A} \qquad (1)$$

where the electrolyte conductivity is $\kappa$, the working gap is $s$ and $A$ is the cross-sectional area of the electrolyte jet at an inner nozzle diameter of 5 mm. The initial electric current $I$ was calculated from the applied voltage $U$ and $R_{\mathrm{Jet}}$ according to the equation (2).

$$I = \frac{U}{R_{\mathrm{Jet}}} \qquad (2)$$

The initial current of the process is calculated without consideration of the influence of gas bubbles on the resistance of the electrolyte jet to analyze the maximal expected current peak.

## 4. Process phases and resulting jet shapes

The lower images of Figure 2 show the electrical current $I$ as function of the process time $t$ and the upper images show the corresponding shapes of the electrolyte jet.

Before the experiment (without applied voltage) the jet is characterized by a uniform shape (Figure 2a) with a diameter of 5 mm near the nozzle tip and a diameter of 10 mm at the contact zone near the workpiece surface.

From the investigation at a voltage of 400 V the process was separated into two phases based on the characteristic developments of the electric current (Figure 2b and 2c). The ignition phase (Figure 2b) represents the start of the process, which is characterized by an electric current peak up to 19 A for this experiment. Gas bubbles were formed in the electrolyte jet at the nozzle tip (yellow arrow in Fig. 2b).

Further highspeed-images that are not shown here, revealed that the more gas bubbles were built, they consolidated to a big gas bubble. This leads to the bursting of the gas bubbles and thereby to an interruption of the electrolyte jet. Hence, the current flow was interrupted as can be seen ($I$ = 0 A) from t = 0.019 s until t = 0.168 s in the diagram below. Then the electrolyte jet is formed again and electrical contact between the nozzle and the workpiece surface is re-built.

The gas bubbles are built on the nozzle's inner surface due to the flowing electric current, which leads to the electrolysis of the water and formation of cathodic hydrogen. Anodically formed oxygen gas is purged away over the workpiece surface by the electrolyte flow and thus not cognizable in the camera images.

During the subsequent polishing phase shown in Figure 2c, random fluctuations of the current were determined. Here, an average electric current of 0.35 A and random peaks from 2 A to 4 A were measured, which corresponds to [11]. The fluctuations of the current also correspond to the results of Parfenov et al. [16] for PeP, where it was classified as the electric hydrodynamic mode. It is assumed, that this mode is also achieved here in the second phase for Jet-PeP, where a polishing process is possible.

The electrolyte jet is characterized by irregularly distributed gas bubbles and evaporation. The evaporation is hardly visible in the high-speed images but could be observed in the process chamber. The gas bubbles were generated by the Joule heating of the electrolyte due to the passed electric current and by the electrolysis of water.

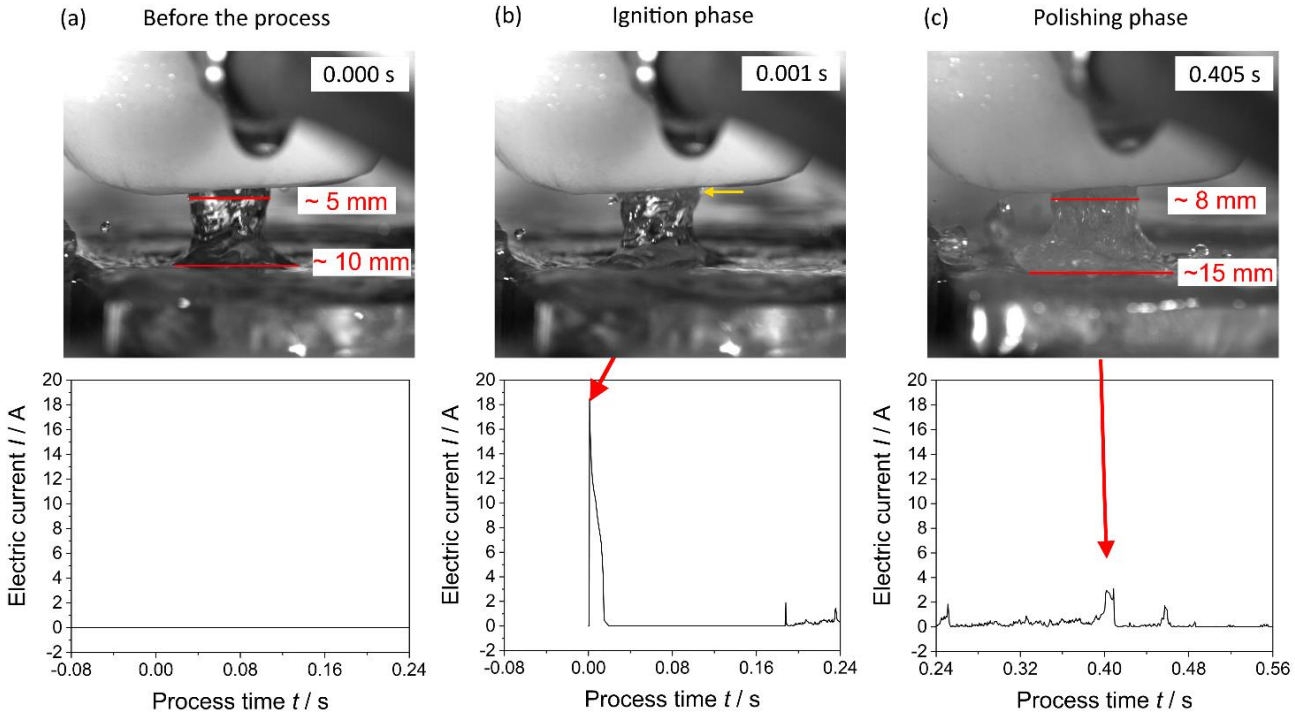


Figure 2. Electric current *I* as a function of the process time *t* for (a) before the process, (b) ignition phase and (c) polishing phase of the Jet-PeP process for a working gap of 6 mm, electrolyte flow rate of 200 ml/min and a voltage of 400 V.

Thus, the electrolyte jet was expanded to a diameter of 8 mm at the nozzle tip and to 15 mm in the near of the workpiece surface. The deformed surface of the jet corresponds with the results in [13].

This results in a ratio of 1.6 between the jet diameter on the anode and the diameter on the cathode. The ratio was also discussed by Popov et al. [9]. The shape of the electrolyte jet in this study is comparable to a truncated cone with an irregular surface. This also corresponds to the results of Popov et al. [9] at comparable voltages in the range from 420 V to 500 V.

The contact between the electrolyte jet and the workpiece surface depends on the applied voltage as shown in Figure 3.

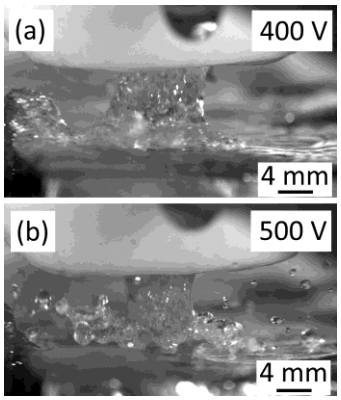


**Figure 3.** Contact between electrolyte jet and sample surface at the polishing phase for (a) 400 V and (b) 500 V.

At 400 V, the shape of the electrolyte jet was a truncated cone during the polishing phase (Figure 3a). Large gas bubbles led to an expansion of the jet. In contrast to this, the contact between the electrolyte jet and the workpiece surface was interrupted at 500 V (Figure 3b). This led to a recurrent pulsation of the electric current, because the interrupted contact led to interruption of the electric current. The gas bubbles are smaller and the jet looks like milky. The reason is the higher electric power and the associated higher Joule heating of the electrolyte jet.

Initiation experiments with a working gap increased to 10 mm revealed that reliable initiation of the Jet-PeP process and the formation of a well-shaped electrolyte jet is only possible with an electrolyte flow rate of 250 ml/min. Furthermore, the increased working gap leads to a higher resistance of the electrolyte jet and therefore a higher voltage is required for the initiation of the Jet-PeP process.

Figure 4 shows the electric current peaks of the ignition phase with the orange bars representing the calculated values according to Eq. 1 and Eq. 2. The measured electric current peaks are displayed by the green bars. It can be stated that all the measured electric current peaks at working gap of 6 mm (Figure 4a) are higher than the calculated ones. The reason for this systematic deviation could be that the formation of gas bubbles led to a higher resistance of the electrolyte jet. The electric power required for the process initiation increased from 5 kW at 300 V to 23.2 kW at 600 V.

At increased working gap of 10 mm shown in Figure 4b, significantly lower electric currents were measured for the investigated voltages due to the higher resistance of the electrolyte jet.

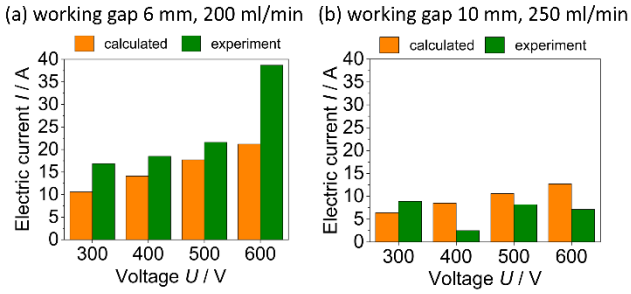


**Figure 4.** Comparison of the calculated (orange bar) and measured (green bar) electric current *I* at the beginning of the process for (a) working gap of 6 mm and electrolyte flow rate 200 ml/min and (b) working gap of 10 mm and electrolyte flow rate 250 ml/min.

Significant initiation current peaks were determined at 300 V and 600 V, but not for 400 V as can be retraced by the lower value. The reason could not be clear determined with the highspeed images. Therefore, further investigations are required to understand the ignition phase of the process.

The results indicate that the calculation of the current peaks deviates systematically from the measured current peaks towards higher values since the simplified calculations do not consider the electric current required for electrolysis and the formation of gas bubbles. Gas bubbles also lead to a lower electrolyte conductivity and hence to a higher electric resistance of the electrolyte jet.

## 5. Luminescence of the electrolyte jet

Figure 5 shows the luminescence of the electrolyte jet at 600 V and a working gap of 6 mm.

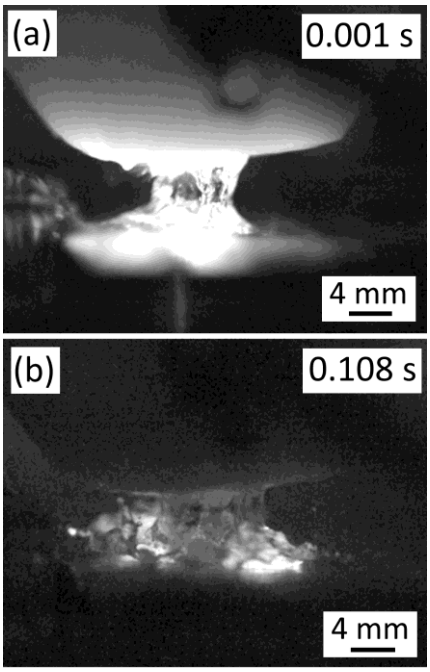


**Figure 5.** Luminescence of the electrolyte jet (a) at the beginning of the process and (b) during the process in the polishing phase at 600 V.

A luminescence was detected in the whole jet (Figure 5a) at a process time of 0.001 s, which came along with an acoustic bang. This indicates an arc discharge, but a crater could not be detected on the workpiece surface. The measured electric current peak of 38.7 A represents an electric power consumption of 23.2 kW at this moment. This led to a heat energy of 23.2 J and additionally heating of the electrolyte jet with the assumption that 100 % are used for the Joule heating.

A luminescence with less intensity, as shown in Figure 5b, in the electrolyte on the surface was observed at 0.108 s after initiation during the polishing phase. In this phase an average electric current of 0.38 A was determined. The luminescence in the truncated cone base was also detected by Popov et al. [9]. Thus, it is expected that a similar process was achieved.

The repeating luminescence of the electrolyte jet during the ongoing polishing process was only observed on the workpiece surface and not on the nozzle tip. According to Popov et al. [9], the luminescence is caused by the recombination of ions of the workpiece material. Another possible mechanism is described in [14] as an ionization of water by highly energetic cations, which are accelerated towards the gas-electrolyte interface.

Due to this fact, it can be derived that electrochemical and physical reactions occur during the Jet-PeP process.

## 6. Conclusion

It was shown that the Jet-PeP process can be separated into two phases based on the measured electric current and the specific luminescence of the electrolyte jet. Here, the ignition phase is characterized by a high current peak and the polishing phase by a comparatively small electric current with random noise.

It was found that the shape of the electrolyte jet was influenced by gas bubbles formed due to electrolysis of the aqueous electrolyte as well as boiling due to Joule heating depending on the flow of electric current. This led to interruptions of the contact between the electrolyte jet and the workpiece surface, which were detected by temporary interruptions of the current flow. The process is characterized by the interaction of the electrochemical and physical reactions.

## Acknowledgment

The research presented in this work was carried out within the Jet-PeP project. The Jet-PeP project is managed by the Project Management Agency Karlsruhe (PTKA) and sponsored by the German Federal Ministry of Education and Research (BMBF) as German-Israeli cooperation in applied nanotechnology under grant number 02P17W010.

## References

[1] "MatWeb Material Property Data." Available: http://www.matweb.com/index.asp?ckck=1. [01-Nov-2020]

[2] H. Zhao, J. Van Humbeeck, J. Sohier, I. De Scheerder, 2002, *J. Mater. Sci. Mater. Med.*, **13**, no. 10, pp. 911–916

[3] D. Loaldi, M. Kain, G. Tosello, 2019, In: Joint Special Interest Group meeting between euspen and ASPE Advancing Precision in Additive Manufacturing

[4] H. Zeidler, F. Boettger-Hiller, J. Edelmann, A. Schubert, 2016, *Procedia CIRP*, **49**, pp. 83–87

[5] K. Nestler, F. Böttger-Hiller, W. Adamitzki, G. Glowa, H. Zeidler, A. Schubert, 2016, *Procedia CIRP*, **42**, no. ISEM Xviii, pp. 503–507

[6] E. V. Parfenov, R. R. Nevyantseva, S. A. Gorbatkov, 2005, *Surf. Coatings Technol.*, **199**, no. 2-3 SPEC. ISS., pp. 198–204

[7] S. Quitzke, A. Martin, A. Schubert, 2020, *16th Intern. Symp. on Electrochem. Machining Technol.*, pp. 181–188

[8] M. F. Akhatov, R. R. Kayumov, R. R. Mardanov, I. I. Saifutdinova, 2020, *J. Phys. Conf. Ser.*, **1588**, no. 1

[9] A. I. Popov, V. I. Novikov, M. M. Radkevich, 2019, *High Temp.*, **57**, no. 4, pp. 447–457

[10] I. I. Galimzyanov, A. F. Gaisin, I. T. Fakhrutdinova, E. F. Shakirova, M. F. Akhatov, R. R. Kayumov, 2018, *High Temp.*, **56**, no. 2, pp. 296–298

[11] A. I. Shaidullin, A. I. Kuputdinova, L. I. Akhmadullina, A. F. Gaysin, F. M. Gaysin, A. F. Gaysin, 2020, *J. Phys. Conf. Ser.*, **1588**, p. 012011

[12] D. N. Mirkhanov, A. F. Gaisin, A. I. Kuputdinova, R. A. Mukhametov, 2017, *J. Phys. Conf. Ser.*, **927**, no. 1, pp. 3–7

[13] A. F. Gaisin,N. F. Kashapov, 2018, *J. Appl. Mech. Tech. Phys.*, **59**, no. 4, pp. 591–593

[14] A. Yerokhin, V. R. Mukaeva, E. V. Parfenov, N. Laugel, A. Matthews, 2019, *Electrochim. Acta*, **312**, pp. 441–456

[15] S. Quitzke, O. Kröning, A. Martin, M. Hackert-Oschätzchen, H.-P. Schulze, C. Kranhold, H. Zeidler, A. Schubert, 2018, *In: Proceedings of the 14th Intern. Symp. on Electrochem. Machining Technol., pp. 63-71*

[16] E. V. Parfenov, R. R. Nevyantseva, S. A. Gorbatkov, 2005, *Surf. Coatings Technol.*, **199**, no. 2-3 SPEC. ISS., pp. 189–197